Materials Letters 211 (2018) 254–257

Contents lists available at ScienceDirect

Materials Letters

journal homepage: www.elsevier.com/locate/mlblue

Porous TiO_2/Fe_2O_3 nanoplate composites prepared by de-alloying method for Li-ion batteries

Weimin Zhao [a,b], Pengyang Fei [a], Xiaomin Zhang [a], Yongguang Zhang [a,*], Chunling Qin [a], Zhifeng Wang [a,b,*]

[a] School of Materials Science and Engineering, Research Institute for Energy Equipment Materials, Hebei University of Technology, Tianjin 300130, China
[b] Key Lab. for New Type of Functional Materials in Hebei Province, Hebei University of Technology, Tianjin 300130, China

ARTICLE INFO

Article history:
Received 7 July 2017
Received in revised form 28 September 2017
Accepted 5 October 2017
Available online 5 October 2017

Keywords:
Li-ion battery
Anode
De-alloying
TiO_2/Fe_2O_3 composite
Nanocomposites
Energy storage and conversion

ABSTRACT

TiO_2 anode presents a stable cycling performance but relatively low theoretical capacity, which has hindered its applications in high-performance Li-ion batteries (LIBs). For improving the Li storage properties, novel TiO_2/Fe_2O_3 composite with a porous "slice on slice" structure was prepared via a facile de-alloying method. The composite delivers a reversible capacity of 838.8 mAh g^{-1} after 400 cycles at a current density of 200 mA g^{-1} and maintaining a discharge capacity of 339 mAh g^{-1} even at 2 A g^{-1}. The improved Li storage property could be ascribed to the synergistic effects of the two active materials. Especially, the reduction products of Fe^0 at the interface between TiO_2 and Fe_2O_3 can facilitate the reversibility of reactions and further result in a high reversible capacity.

1. Introduction

As one of the most prominent electrical energy storage devices, Li-ion batteries (LIBs) are widely used due to their high energy density and long cycling life [1]. As a possible anode material of LIBs, TiO_2 exhibits both an efficient rate and stable cycling performance [2]. However, it is well known that TiO_2 possesses a relatively low theoretical capacity of 335 mAh g^{-1}, which has seriously hindered their practical applications in high-performance LIBs [3]. Currently, composite metal-oxide anodes, which consist of two active materials with synergistic effects and improved Li storage properties, have attracted increasing interest [4]. A number of metal oxides with high specific capacity of above 500 mAh g^{-1} were used to synthesize TiO_2 based composites. For example, Chen et al. [5] investigated the electrochemical performance of core-shell $CuO@TiO_2$ nanorods, which delivered a reversible capacity (400 mAh g^{-1} at 0.1 C) and stable cyclability (97% after 100 cycles). A sandwich-like Co_3O_4/TiO_2 composite [6] was fabricated through a hydrothermal method and used as anode materials for LIBs, showing excellent electrochemical performance with capacity retention of 668 mAh g^{-1} after 120 cycles at 100 mA g^{-1}.

Despite the observed benefits of binary composite anodes, the nanostructured composites often required the use of complex synthesis processes. Among these methods, de-alloying has been demonstrated to be relatively facile method to prepare transition metal oxides by carefully designing the components of the precursor alloy [7]. In the current work, TiO_2/Fe_2O_3 composites with porous structure were obtained by de-alloying of $Fe_4Ti_2Al_{94}$ precursor alloy. The composites show the prospective applications as an advanced anode for LIBs with a good rate capability and excellent cycling performance, which could be ascribed to the synergistic effects of Fe_2O_3 and TiO_2 [8,9].

2. Experimental

$Fe_4Ti_2Al_{94}$ (at%) ingots were prepared by refining high purity Al, Ti and Fe (99.99 wt%) in a vacuum arc furnace. Alloy strips with about 20 μm in thickness and 3 mm in width were then fabricated through melt-spinning process [10]. The dealloying was performed by etching Al from alloy strips (3 g each group) accompanied by spontaneous oxidation in 2 L 2 M NaOH solutions at 25 °C for 12 h. After washed three times with ultra-pure water (18.2 MΩ cm) and dried in vacuum oven (−0.08 MPa) at 60 °C for 24 h, the

---

* Corresponding authors at: School of Materials Science and Engineering, Research Institute for Energy Equipment Materials, Hebei University of Technology, Tianjin 300130, China.

E-mail addresses: yongguangzhang@hebut.edu.cn (Y. Zhang), wangzf@hebut.edu.cn (Z. Wang).

https://doi.org/10.1016/j.matlet.2017.10.019
0167-577X/© 2017 Published by Elsevier B.V.

TiO_2/Fe_2O_3 composites were finally obtained as active materials for LIB anodes.

The phases were analyzed with an X-ray diffractometer (XRD) using Cu Kα radiation. The morphology of the oxides were observed by scanning electron microscopy (SEM). The specific surface area was calculated using the Brunauer-Emmett-Teller (BET) method. X-ray photoelectron spectroscopy (XPS) was carried out to establish the valence states of surficial elements.

For the preparation of the working electrode, a mixture of active materials, Ketjen black and carboxymethyl cellulose binder with a weight ratio of 7:2:1 was dispersed in ultrapure water and milled for 30 min. The resulting slurry was evenly spread on the copper foil and dried at 60 °C for 24 h under vacuum. The load of active materials was about 0.8 mg cm^{-2}. 1 M $LiPF_6$ in ethylene carbonate/dimethyl carbonate (1:1, v/v) was used as the electrolyte. Disc-shaped Li foil were used as both counter electrode and reference electrode, and Celgard 2400 was used as the separator. The coin-type cells (CR 2032) were assembled in an argon-filled glove box. The charge-discharge tests were performed by using a battery testing system (LAND CT2001A, China) at room temperature. The cyclic voltammetry (CV) test was carried out on an electrochemical workstation (Princeton Applied Research, PARSTAT 2273).

3. Results and discussion

SEM images of the de-alloyed sample are shown in Fig. 1a. It is clearly observed that the resulting sample consists of a large quantity of the slices, which are in regular with edge lengths between 1–3 μm and thickness around 50 nm. The SEM image with higher magnification in Fig. 1b depicts the detailed structure of the sample. By etching Al atoms with NaOH solutions, the Ti and Fe atoms undergo direct oxidization in the solution. The robust Fe_2O_3 nanoplates were formed and coated by small-sized TiO_2 nanoplates, which formed a slice on slice structure with plentiful voids. The element mapping demonstrated in Fig. 1c–f revealed that the elements of Fe, Ti and O distribute across the whole structure, indicating the componential uniformity of the TiO_2/Fe_2O_3 nanoplates. Fig. 1 g shows the nitrogen adsorption-desorption isotherms for the samples. The isotherms show type IV hysteresis loops, which indicates the mesoporous nature of our sample. We believe the type IV hysteresis loop stems from the aggregated nanosheets-like structure [11]. The BET surface area for TiO_2/Fe_2O_3 samples was 209.19 m^2 g^{-1}. The results of BET analysis aligned well with the SEM study. Insets shows the BJH pore size adsorption plot for TiO_2/Fe_2O_3 sample, revealing that the nano-composite possess a mono-pore size of around 6.7 nm.

Powder XRD was used to examine the crystal structure of the resulting samples after dealloying. As shown in Fig. 2a, no obvious diffraction peak emerged, indicating the weak crystallinity of the de-alloyed sample. The low-intensity peaks can be assigned to Fe_2O_3 (JCPDS 39-1346) and TiO_2 (JCPDS 21-1272) species. In order to further confirm the oxidation states of metal elements in the de-alloyed sample, XPS analysis was carried out. Fig. 2b–d presents the Fe 2p, Ti 2p and O 1 s core level spectra for the dealloyed materials. As shown in Fig. 2b, the peaks of Fe $2p_{3/2}$ and Fe $2p_{1/2}$ located at 711.2 and 725 eV, with an energy separation of 13.8 eV, are in good agreement with the reported data of the Fe_2O_3 [9]. Similarly, as shown in Fig. 2c, two main peaks of Ti located at 458.3 eV for $2p_{3/2}$ and 464.1 eV for $2p_{3/2}$ matched well with the typical binding energy values of TiO_2 [9]. The peak observed at 530 eV is attributed to OM oxygen, corresponding to O^{2-} ions in transition metal oxide, as shown in Fig. 2d. The above results confirmed that Fe_2O_3 and TiO_2 co-exist in the de-alloyed sample. Moreover, the XPS results further showed that the atom ratio of the TiO_2/Fe_2O_3 is about 1:1.2. The content of residual Al is about 5.82 at%, indicating an incomplete dealloying.

Cyclic voltammogram of the TiO_2/Fe_2O_3 composite in the first three cycles were investigated at a scan rate of 0.1 mV s^{-1} of 0.01–3 V at room temperature. As seen in Fig. 3a, two reduction peaks around 1.3 V and 0.6 V are resulted from the insertion of Li into the TiO_2/Fe_2O_3 and complete reduction of Fe_2O_3 to metallic Fe and SEI film formation, respectively. For the anodic scan, oxidized peaks centered around 1.0–2.0 V correspond to the reversible process, including oxidation of Fe^0 to Fe^{2+} and Fe^{2+} to Fe^{3+}, delithiation of Li_xTiO_2 as well as the conversion of Li_2O [8,12]. Fig. 3b shows the charge/discharge voltage profiles of the

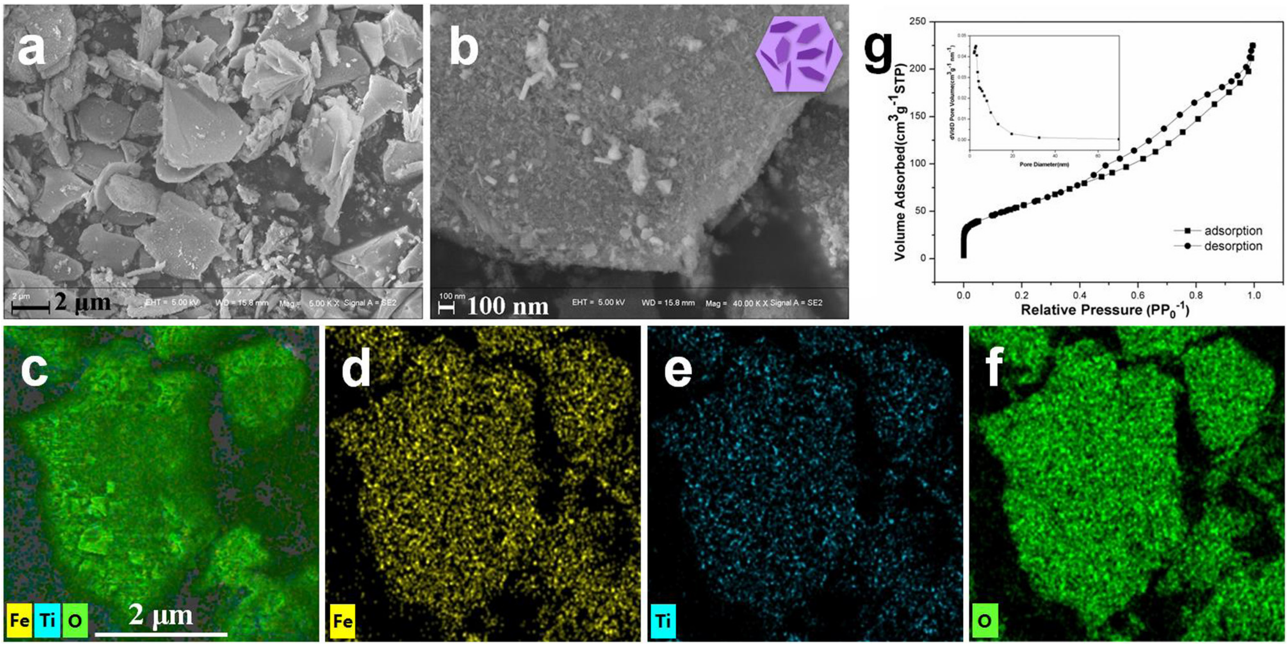

Fig. 1. (a–b) SEM images of the de-alloyed $Fe_4Ti_2Al_{94}$ strips. (c–f) Element mapping of TiO_2/Fe_2O_3 nanoplates: (c) combined image, (d) Fe, (e) Ti and (f) O. (g) Nitrogen adsorption/desorption isotherms of TiO_2/Fe_2O_3, insets: pore size distributions.